PHYSICS DESIGN FOR THE C-ADS MAIN LINAC BASED ON TWO DIFFERENT INJECTOR DESIGN SCHEMES*

Fang Yan, Zhihui Li, Cai Meng, Jingyu Tang,
Institute of High Energy Physics, Chinese Academy of Science, Beijing, 100049, China

Abstract

The China ADS (C-ADS) project is proposed to build a 1000-MW Accelerator Driven sub-critical System around 2032. The accelerator will work in CW mode with 10 mA in beam current and 1.5 GeV in final beam energy. The linac is composed of two major sections: the injector section and the main linac section. There are two different schemes for the injector section. The Injector-I scheme is based on a 325-MHz RFQ and superconducting spoke cavities of same RF frequency and the Injector-II scheme is based on a 162.5-MHz RFQ and superconducting HWR cavities of same frequency. The two different designs for the main linac have been studied according to the different beam characteristics from the injector designs.

INTRODUCTION

The China ADS project is proposed to build a 1000-MW Accelerator Driven sub-critical System around 2032. The driver accelerator will work in CW mode, with a beam of 1.5 GeV in final energy and 10 mA in beam current. The C-ADS linac includes two major sections: the injector section and the main linac section. According to the very strict requirements of high reliability and availability for the ADS application [1], the C-ADS linac adopts two parallel injectors design, with one as the hot-spare of the other. Another redundancy or fault-tolerance design is the application of the so-called local compensation method in the main linac part which allows failures of key components such as cavities and focusing elements. The injectors accelerate the proton up to 10 MeV and the main linac boost the energy from 10 MeV up to 1.5 GeV, and a section of beam line named MEBT2 [2] is applied to transfer and match the beam from the two injectors to the main linac. The general layout of the linac is shown in Figure 1.

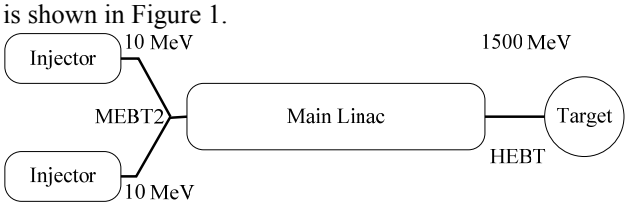

Figure 1: Layout of the C-ADS linac.

At present, two different design schemes for the injectors are proposed [3, 4], with Scheme I based on 325 MHz and Scheme II based on 162.5 MHz. For both design schemes, the injector is composed of an ECR ion source, a LEBT, a RFQ, a MEBT1 and a superconducting section. There will be a matching section – MEBT2 to transfer the beam from any of the two injectors to the main linac. The beam parameters at the exit of the injectors for the two schemes are listed in Table 1.

Table 1: Beam Parameters at the Exit of the Injectors

Parameters	Scheme I	Scheme II
Frequency /MHz	325.0	162.5
α /x/y/z	-1.21/-1.19/0.10	-0.34/-0.37/0.27
β /x/y/z / mm/pi.mrad	2.43/2.34/1.03	0.82/0.84/2.08
ε_t /mm.mrad	0.20	0.32
ε_l /mm.mrad	0.17	0.37

The beam parameters at the exit of the two injector design schemes are quite different. The difference on the Twiss parameters is not so important for the design of the main linac, since the MEBT2 will match the beam to the main linac. But the differences on bunch frequency and emittances will affect the structure of the main linac significantly. With same beam current, the different bunch frequency means different bunch intensity and different space charge effect. This will ask for different lattice structures to obtain a stable beam dynamics design. The frequency jump in the front of the main linac will ask for a larger longitudinal acceptance and cause potential troubles in longitudinal beam dynamics. The different emittance means difference in the acceptance and in the ratio of longitudinal and transverse phase advances. This paper will present the design considerations of the main linac based on two injector design schemes.

GENERAL CONSIDERATIONS ON THE MAIN LINAC DESIGN

In order to satisfy the rigorous demands on the accelerator stability and reliability, over-design, redundancy and fault tolerance strategies are implemented in the basic design. The fault tolerant design in the main linac is guaranteed by means of the local compensation and rematch method [5], which is effective only for a linac composed of short independently powered cavities. To cover the whole energy range of from 10 MeV to 1.5 GeV in the main linac section, we need at least four types of superconducting cavities. After optimization, we have chosen two single-spoke cavities working at 325 MHz with geometry betas of 0.21 and 0.40, respectively, and two 5-cell elliptical cavities working at 650 MHz with geometry betas of 0.63 and 0.82, respectively. The acceleration efficiencies of the four cavities and their effective energy ranges are shown in Figure 2. The effective energy ranges for the four types of cavities are all shifted to the lower energy to accommodate the special phase advance law required by the stable beam dynamics. The parameters of the cavities are listed in Table 2. For

*Work supported by Advanced Research Project of CAS
yanfang@ihep.ac.cn

ISBN 978-3-95450-118-2

the nominal design, only 2/3 of the maximum cavity voltage is used, whereas another 1/3 is reserved for the local compensation, and this redundancy also benefits the cavity reliability.

The lattice structures for each section of the main linac are shown in Figure 3, and they are characterized by long drift in both side of each period. With this kind of lattice structure, the cryomodule structure is more flexible. It can accommodate one period, two periods or even more periods without affecting the beam dynamics performance and is totally decided by the mechanical and engineer considerations. Furthermore, it also helps in minimizing the possibility of mismatch within one section. The matching between two sections is guaranteed by varying the parameters of the adjacent cavities and transverse focusing elements.

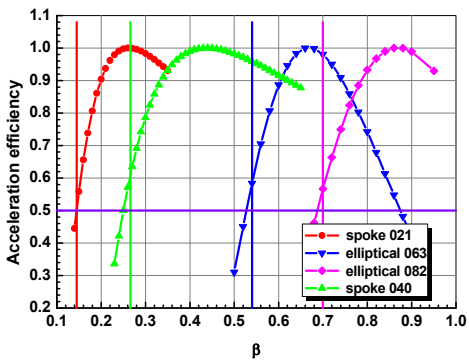

Figure 2: Acceleration efficiency of the cavies in main linac.

Table 2: Parameters of the Cavities in the Main Linac

Cavity type	βg	Freq. MHz	Vmax MV	Emax MV/m	Bmax mT
S-Spoke	0.21	325	1.64	31.14	65
S-Spoke	0.40	325	2.86	32.06	65
5-cell ellip.	0.63	650	10.26	37.72	65
5-cell ellip.	0.82	650	15.63	35.80	65

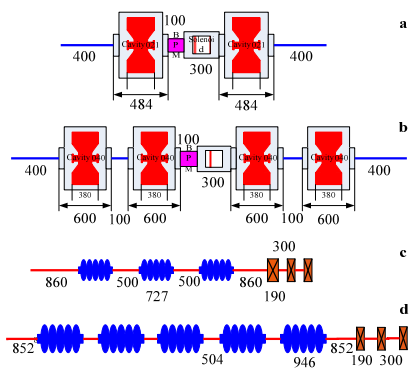

Figure 3: schematic view of the lattice structures for the main linac sections.

The phase advances per cell in all the three phase planes are usually kept below 90° to avoid the parametric resonance [6]. Except for the matching cells at the section transitions, the focusing fields in both the transverse and longitudinal directions are kept constant in each section to have almost constant envelope amplitude when the geometry emittance is shrinking along the acceleration [7]. This also means constant synchronous phase in each section, but the absolute value of the synchronous phase decreases from lower energy section to higher energy section to obtain higher acceleration rate while maintaining the acceptance and emittance ratio larger than 10, a low beam loss design criteria for the acceptance in the main linac. Due to the limitation in the longitudinal phase advance per cell, the cavity voltages at the beginning parts of the sections may not be fully exploited.

Since the phase advance per cell should be below 90° , it is better to set the longitudinal phase advance larger than transverse one to obtain higher acceleration efficiency. When longitudinal emittance is smaller than the transverse one, then the transverse focusing parameters along the linac can be determined by the equipartition condition to avoid the energy transfer between different freedoms. When longitudinal emittance is larger than the transverse, the equipartition condition cannot be fulfilled, but as Hoffman suggested we can set the working point at the resonance-free region in the Hofmann chart [8]. Then even with free energy, no mechanism will drive the energy exchange between different freedoms.

Among the three transitions for the four sections of different lattice structures and cavity types, the one between the section Spoke040 and the section Ellip063 is the most critical. One reason is the RF frequency doubling from Spoke040 to Ellip063, and the other is the transverse focusing from inside-cryomodule solenoids to warm triplet quadrupoles. Careful matching should be carried out to avoid important emittance growth at all the transitions. One method is to make smooth focusing changes, and another method is to avoid the absolute synchronous phase being too small.

MAIN LINAC DESIGN BASED ON INJECTOR SCHEME I

The block diagram of the main linac based on injector scheme I is shown in Figure 4. It is composed of four sections: Spoke021 section, Spoke040 section, Ellip063 section and Ellip082 section.

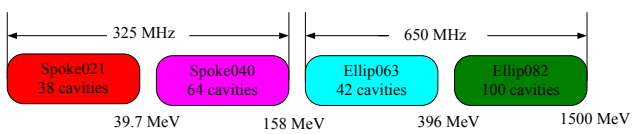

Figure 4: Block diagram of the main linac based on injector scheme I.

General Design

The design follows the general design considerations in the last section. Different phase advance ratios between

ISBN 978-3-95450-118-2

the longitudinal and the transverse planes have been studied. It turns out that the phase advance ratio of 0.75 is adopted after the compromise among the equipartitioning condition, the acceptance to emittance ratio and the phase advances per cell. Figure 5 shows the tune footprint in the Hofmann chart. We can see except one point falling in very weak part of the k_z/k_x=2 resonance region, all the other points are in the resonance-free region.

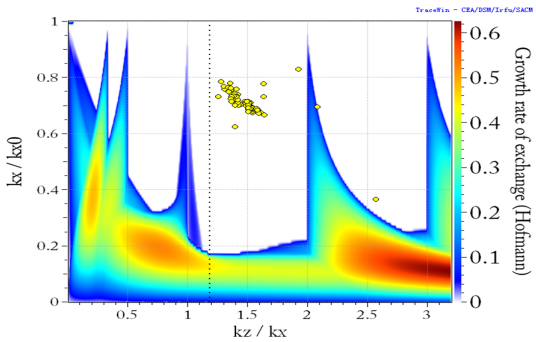

Figure 5: Tune footprint in the Hofmann chart.

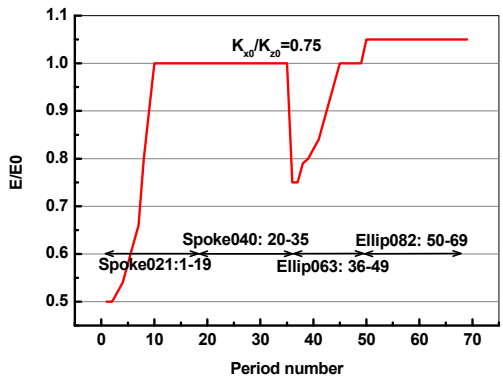

Figure 6: Effective RF voltage in use as compared with the nominal voltage.

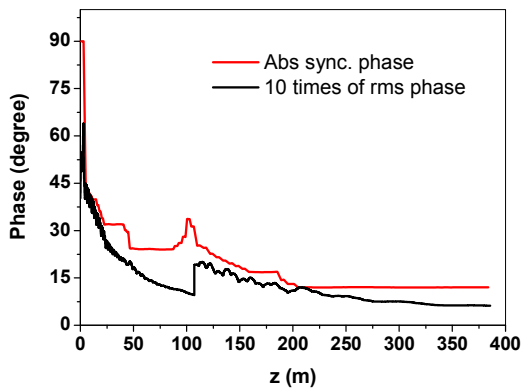

Figure 7: The absolute synchronous phase and 10 times RMS phase width along main linac.

Figure 6 shows the effective RF voltage in use as compared with the nominal voltage for all the four types of superconducting cavities. It is the optimized results by following the requirements on the phase advance, smooth change in focusing and longitudinal acceptance. Another limitation on the effective field level comes from the multipacting effect in the superconducting spoke cavities. The voltage ratio should not be lower than 0.5 to avoid the possibility of working in the multipacting regions. To reduce beam loss, the synchronous phase is kept larger than 10 times the RMS phase width throughout the main linac as shown in Figure 7. The phase advance per meter is shown in Figure 8 and it changes quite smoothly

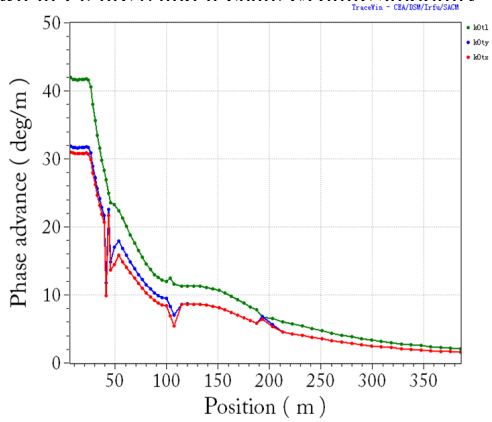

Figure 8: Phase advances per meter along the main linac.

Multi-Particle Simulations

For the multi-particle simulations, it is important to include space charge forces and specify the initial beam distribution. Although most studies use a 6D parabolic distribution, other distributions such as truncated Gaussian distribution and simulated distributions at the injectors exit should be also used to check the design robustness. As the first step, we have studied the dynamic behaviour of the beam core or the properties in RMS along the linac. The emittances at the exit of RFQ are 0.21 πmm.mrad in the transverse planes and 0.18 πmm.mrad in the longitudinal plane, respectively, but an emittance growth of about 20% is assumed in the injector and in the MEBT2 section. Without taking into account all kinds of errors and with an input 6D parabolic distribution of 10^5 macro-particles, the multi-particle simulations for the whole main linac section have been carried out. It is found that the transverse emittance growths are 3% and 2.8% for the horizontal and vertical planes, respectively, and the longitudinal emittance growth is -0.3%. The transverse RMS beam size in average is about 2.5 mm. The evolution of the normalized RMS emittance along the main linac is shown in Figure 9.

From the simulation results, we can find that the rms emittance growth along the main linac is under control in all the three phase spaces, e.g. about a few per cent. The envelope evolution is also smooth along the linac. The tune depressions in the three planes remain as about 0.72 along the linac, and are situated in the transition phase between the space-charge dominant regime and the emittance dominant regime.

The multi-particle simulations with 20 mA, which corresponds to the injector-II scheme with the same emittances, are also performed. The basic lattice design

ISBN 978-3-95450-118-2

remains the same, only the matched input Twiss parameters and the matching between the sections are revised. The simulation results using a 6D parabolic distribution of 1×10^5 macro-particles show that the RMS emittance growth along the linac is still under control but clearly larger than that with the beam current of 10 mA, and the envelope evolution is also not as smooth as the 10-mA design.

The error analysis of the design is also performed and details can be found in [4].

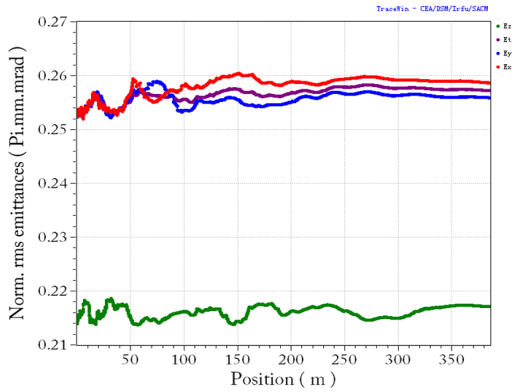

Figure 9: Normalized RMS emittances along the main linac.

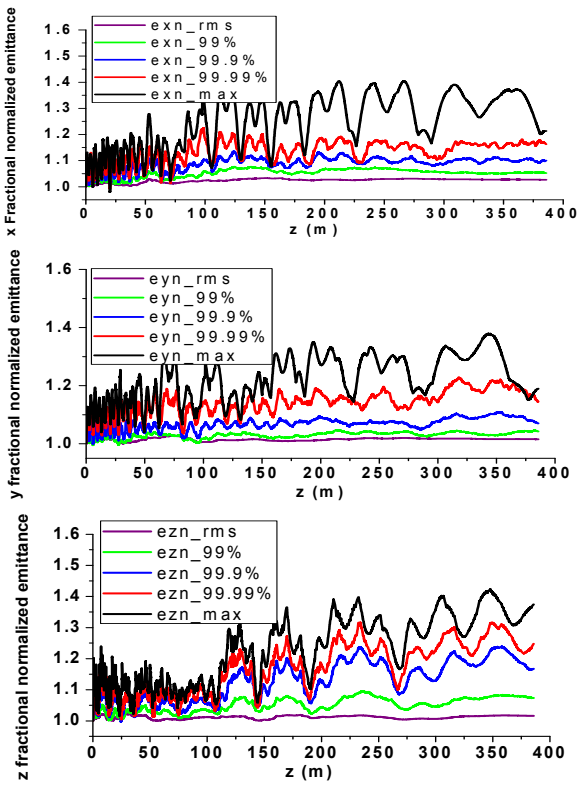

Figure 10: Halo development along the main linac for different beam fractions.

Halo Formation Studies

As the halo development due to errors, mismatches and resonances is the key causing beam loss, it becomes the central focus of the beam dynamics studies once the lattice and the basic dynamic behaviour are determined using the beam core or the RMS emittance. As this is a linac of very high beam power, beam loss should be controlled at the level of 10^{-8}/m at high energy part. This means that the behaviours of very sparse halo particles should be studied. Therefore, the emittance evolutions for 99%, 99.9%, 99.99% and 100% beam fractions have been studied, using both TRACK [9] and TraceWin [10] codes. The number of macro-particles is 10^5 for the simulations.

For the halo development related to the space charge resonances, we have carried out simulations on the halo formation to see if the working point is sensitive or not. Figure 10 shows the emittance evolutions with the nominal working point ($\varepsilon_z/\varepsilon_x$=0.85, k_x/k_z=0.75), which is free from dangerous resonances. The emittances with different fractions of particles indicate that the basic design is robust.

The halo formation with double bunch current is also studied. It indicates that the maximum emittance growth is about two times the one with 10 mA, which shows the injector scheme of higher RF frequency is favoured from the beam dynamics point of view.

MAIN LINAC DESIGN BASED ON INJECTOR SCHEME II

The main differences between the two injector schemes are the bunch frequency and emittances. If we examine the previous main linac design with the output beam parameters obtained up to now from the injector scheme II studies, we find the acceptance criteria is violated if the field level and the phase advances laws are followed. The main reason is that the longitudinal emittance is much larger here. In order to solve this problem, an alternate design modified from the previous design for injector scheme II is proposed.

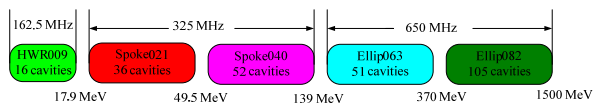

Figure 11: Block diagram of main linac design based on injector scheme II.

Base Line Design

As shown in Figure 11, the main linac on basis of Injector II scheme is composed of five sections. Besides the four sections as used in the previous design, an additional HWR section with the same cavity type as in the injector is added in front of Spoke021 section. The lattice structure of the HWR section is similar as the Spoke021 section: each period is composed of two superconducting cavities, one solenoid and one BMP. By adding this section, the frequency jump is shifted to higher energy (17 MeV), and the longitudinal acceptance condition can be met while keeping the peak field of Spoke021 cavity Ep>12.5MV/m to avoid multipacting effects. The design results such as synchronous phase, zero current phase advances per period are shown in Figures 12 and 13, respectively.

ISBN 978-3-95450-118-2

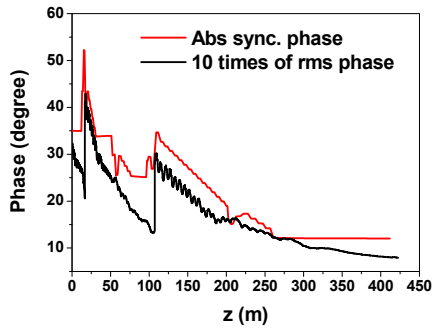

Figure 12: Synchronous phase and 10 times RMS phase width along the main linac with injector scheme II.

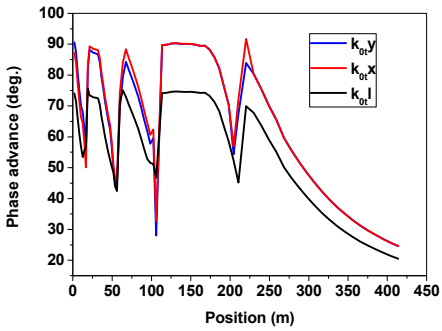

Figure 13: Evolution of transverse (red and blue) and longitudinal (green) phase advances.

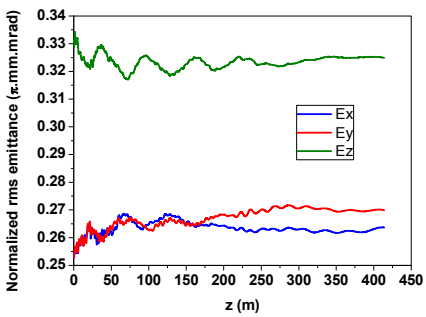

Figure 14: Normalized rms emittance growths along the main linac with injector scheme II.

Beam Dynamics Simulations

The beam dynamics programs used for the simulations are TraceWin and Track. The transverse and longitudinal emittance at the exit of RFQ are 0.210 πmm.mrad and 0.273 π mm.mrad, respectively. An emittance growth of about 20% is assumed in the injector and MEBT2 section. Without taking into account all kinds of errors and with an input 6D parabolic distribution of 10^5 particles, the multi-particle simulations for the whole main linac section have been carried out. As shown in Figure 14, the transverse RMS emittance growth are 4.3% and 6.7% for the horizontal and vertical, respectively, the longitudinal emittance growth is -1.1%. From the simulation results, it is find that the RMS emittance growth along the linac is under control in all the three phase spaces, e.g. a few percent. The beam halo information is also studied. The 100% emittance growths are under 95%, 120% and 70% for horizontal, vertical and longitudinal directions respectively. The relatively larger halo emittance growths are understandable as it is a space charge dominated beam with a bunch current doubled than that with injector I scheme. The envelope evolution is also smooth along the linac and the RMS beam size is about 2 mm.

SUMMARY AND PERSPECTIVE

The C-ADS main linac basic designs and beam dynamics results based on the two injector design schemes have been presented. Longitudinal emittance plays a very important role in designing the lattice structure. The lattices are designed to be conservative to meet the very strict reliability and stability specifications, especially by incorporating the local compensation method. Multi-particle simulations show that the designs are reasonably good in controlling emittance growth and beam losses with errors included.

Much more efforts in further optimization of the lattice by including cost trade-off, end-to-end simulations, design robustness with cavity performance variations and different input beam distributions will be needed in the future.

The authors express their sincere acknowledgement to the colleagues in the C-ADS accelerator team and the members of the international review committees on C-ADS linac for many good suggestions and comments.

REFERENCES

[1] Z. Li et al., "Beam dynamics design of China ADS linac", THO3A2, these proceedings.
[2] Zhen Guo et al., "The MEBT2 Design for the C-ADS", MOP217, these proceedings.
[3] Y. He et al., "The Conceptual Design of Injector II of ADS in China", IPAC'11, San Sebastian, Spain, p.2613.
[4] J.Y. Tang and Z.H. Li, edited, "Conceptual Physics design on the C-ADS accelerator", IHEP-CADS-Report/2012-01E.
[5] B. Sun et al., "Compensation-rematch for major element failures in the C-ADS accelerator", MOP220, these proceedings.
[6] F. Gerigk, I. Hofmann, Beam dynamics of non-equipartitined bams in the case of the SPL project at CERN, Proceedings of PAC2001, Chicago, Illinois USA.
[7] M. Reiser and N. Brown, Proposed High-Current rf Linear Accelerators with Beams In Thermal Equilibrium, Physical Review Letters, 1995, Vol. 74, No. 7, 1111-1114
[8] I. Hofmann, "Dynamical aspects of emittance coupling in intense beams", TUO3A01, these proceedings.
[9] http://www.phy.anl.gov/atlas/TRACK/.
[10] http://irfu.cea.fr/Sacm/en/logiciels/index3.php

ISBN 978-3-95450-118-2